PCP
PLANT & CELL PHYSIOLOGY

Strigolactone Biosynthesis Genes of Rice are Required for the Punctual Entry of Arbuscular Mycorrhizal Fungi into the Roots

Yoshihiro Kobae[1,2,*], Hiromu Kameoka[1,3], Yusaku Sugimura[4], Katsuharu Saito[4], Ryo Ohtomo[2], Toru Fujiwara[1] and Junko Kyozuka[1,5]

[1]Graduate School of Agricultural and Life Sciences, The University of Tokyo, 1-1-1 Yayoi, Bunkyo-ku, Tokyo, 113-8657 Japan
[2]Hokkaido Agricultural Research Center, National Agriculture and Food Research Organization (NARO), 1 Hitsujigaoka, Toyohira-ku, Sapporo, Hokkaido, 062-8555 Japan
[3]Division of Symbiotic Systems, National Institute for Basic Biology, 38 Nishigonaka, Myodaiji, Okazaki 444-8585, Aichi, Japan
[4]Faculty of Agriculture, Shinshu University, Minamiminowa, Nagano, 399-4598 Japan
[5]Graduate School of Life Sciences, Tohoku University, 2-1-1 Katahira, Aoba-ku, Sendai, 980-8577 Japan
*Corresponding author: E-mail, kobaemail@gmail.com; Fax, +81-11-859-2178
(Received November 16, 2017; Accepted December 29, 2017)

Regular Paper

Arbuscular mycorrhiza (AM) is a mutualistic association between most plant species and the ancient fungal phylum Glomeromycota in roots, and it plays a key role in a plant's nutrient uptake from the soil. Roots synthesize strigolactones (SLs), derivatives of carotenoids, and exude them to induce energy metabolism and hyphal branching of AM fungi. Despite the well-documented roles of SLs in the pre-symbiotic phase, little is known about the role of SLs in the process of root colonization. Here we show that the expansion of root colonization is suppressed in the mutants of rice (*Oryza sativa*) SL biosynthesis genes, carotenoid cleavage dioxygenase *D10* and more severely in *D17*. Interestingly, most of the colonization process is normal, i.e. AM fungal hyphae approach the roots and cling around them, and epidermal penetration, arbuscule size, arbuscule number per hyphopodium and metabolic activity of the intraradical mycelium are not affected in *d10* and *d17* mutants. In contrast, hyphopodium formation is severely attenuated. Our observations establish the requirement for SL biosynthesis genes for efficient hyphopodium formation, suggesting that SLs are required in this process. Efficient hyphopodium formation is required for the punctual internalization of hyphae into roots and maintaining the expansion of colonization.

Keywords: Arbuscular mycorrhiza • Hyphopodium • Infection unit • Rice (*Oryza sativa* L.) • Strigolactones.

Abbreviations: AM, arbuscular mycorrhiza; CO, chito-oligosaccharide; d.p.p.days post-planting; DAB, 3,3′-diaminobenzidine; FITC, fluorescein isothiocyanate; HRP, horseradish peroxidase; IU, infection unit; LC-MS/MS, liquid chromatography–tandem mass spectrometry; Myc-LCO, Myc-lipo-chito-oligosaccharide; NBT, nitro-blue tetrazolium; RHB, rhizospheric hyphal branch; RNA-seq, RNA sequencing; RT–PCR, reverse transcription–PCR; SDH, succinate dehydrogenase; WGA, wheat germ agglutinin; WT, wild type.

footnote: Data sets of the short reads in this paper have been submitted to the DDBJ Sequence Read Archive under accession number SSUB006029.

Introduction

Arbuscular mycorrhiza (AM) is a ubiquitous endosymbiosis observed in most terrestrial plant species (Smith and Read 2008). AM fungi help plants to take up nutrients, in particular phosphorus (P), as well as nitrogen (N) and other minerals into the roots (Smith and Smith 2011, Courty et al. 2015). AM fungal propagules occur among many other soil microorganisms, and successful colonization relies on a pre-symbiotic signal exchange that allows specific mutual recognition and subsequent cellular reorganization to internalize the hyphae of AM fungi into roots. If successful recognition occurs, hyphopodia are formed on the root surface to penetrate the roots (Bonfante and Genre 2010); the hyphae spread longitudinally within the roots and form arbuscules, highly branched structures of AM fungi that are regarded as the major sites for nutrient exchange (Harrison 2005) in cortical cells. Increased spatial exploitation by extraradical hyphae in the soil (Marschner 1995) and greater mineral acquisition of mycorrhizal roots enable the host plant to improve nutrition and, in many cases, leads to increased growth in comparison with that under non-mycorrhizal conditions (Smith and Read 2008).

Many studies have illustrated the mechanism of pre-symbiotic chemical cross-talk between roots and AM fungi. Spore germination of AM fungi in the soil and the growth of fungal hyphae are stimulated in the presence of a host root (Mosse and Hepper 1975, Bécard and Fortin 1988, Giovannetti et al. 1994, Buee et al. 2000). A purified sesquiterpene lactone from the root exudates, strigolactone (SL), and the synthetic analog GR24 have been shown to induce hyphal branching and activate the mitochondrial energy metabolism of AM fungi (Akiyama et al. 2005, Besserer et al. 2006, Besserer et al. 2008, Salvioli et al. 2016). In addition, the perception of SLs by germinated spores of *Rhizophagus irregularis* causes an increase in the production of short-chain chito-oligosaccharides (COs; CO4–CO5) (Genre et al. 2013), in turn activating the symbiotic signaling pathway, with Ca^{2+} spiking responses in the root epidermis (Genre et al. 2013, Sun et al. 2015).

Plant Cell Physiol. 59(3): 544–553 (2018) doi:10.1093/pcp/pcy001, Advance Access publication on 9 January 2018, available online at www.pcp.oxfordjournals.org

SLs were originally isolated from plant root exudates as germination stimulants for root parasitic plants of the family Orobanchaceae (Cook et al. 1966, Xie et al. 2010). Recent genetic studies have illustrated that SL biosynthesis proceeds through the isomerization of β-carotene by β-carotene isomerase (D27), followed by cleavage by two carotenoid cleavage dioxygenases (CCD7/D17 and CCD8/D10), which results in the formation of carlactone (Alder et al. 2012, Seto et al. 2014). Carlactone is then converted to SLs by Cyt P450 homologs (MAX1s) (Cardoso et al. 2014, Zhang et al. 2014). In rice, the Max1 homolog Os900 catalyzes the oxidation of carlactone to the first real SL of rice, 2′-*epi*-5-deoxystrigol (*epi*-5DS) (Zhang et al. 2014). SLs are not detected by liquid chromatography–tandem mass spectrometry (LC-MS/MS) in shoots, roots and root exudates of *d17* and *d10* mutants (Umehara et al. 2008) and in roots and root exudates of the pea *ccd8* mutant (Gomez-Roldan et al. 2008). Only minute amounts of SLs are detected in the tomato *ORT1* mutant, in which *CCD7* expression is reduced (Koltai et al. 2010). Accordingly, these mutants or antisense lines exhibit reduced promotion of hyphal branching and root colonization (Gomez-Roldan et al. 2008, Koltai et al. 2010, Vogel et al. 2010, Yoshida et al. 2012). SLs are probably synthesized in the root cortex (Sasse et al. 2015, Borghi et al. 2016) and released into the rhizosphere through hypodermal passage cells mediated by a PDR-type ATP-binding cassette (ABC) transporter (Kretzschmar et al. 2012, Sasse et al. 2015). In the petunia *pdr1* mutant, AM fungal colonization is delayed; however, the morphology of intercellular hyphae and arbuscules is normal (Kretzschmar et al. 2012). In rice *d17* and *d10* mutants, colonization levels are reduced; however, normal arbuscules are observed (Gutjahr et al. 2012). Exogenous application of GR24 to SL-deficient mutants partially restores the colonization level (Gomez-Roldan et al. 2008, Yoshida et al. 2012). These observations suggest that SLs enhance successful mycorrhization on the host (Koltai, 2014, Walter et al. 2015).

In addition to the crucial roles of SLs in pre-symbiotic chemical dialog, genes related to SL signaling are likely to be implicated in the early signaling events of root colonization. The level of *epi*-5DS, the major endogenous SL of rice, is nearly 10 times higher in root exudates of the *d3* mutant than in those of the wild type (WT) under P-deficient conditions (Arite et al. 2009, Umehara et al. 2010). Accordingly, hyphal branches of AM fungi near *d3* roots are markedly increased in comparison with those of the WT (Yoshida et al. 2012). Nevertheless, AM fungal colonization in *d3* roots is severely suppressed (Yoshida et al. 2012, Foo et al. 2013, Gutjahr et al. 2015a). *D3*/*RMS4*/*MAX2* encodes an F-box protein that confers target specificity to the SKP1–CULLIN–F-box (SCF) class of E3 ubiquitin ligase complexes (Stirnberg et al. 2007, Zhao et al. 2014), which conjugate ubiquitin to the target protein. Interactions between D3 and the target protein are activated by SL perception and hydrolysis inside the D14 protein (Yao et al. 2016), leading to the degradation of the target protein by the 26S proteasome and activation of downstream responses to SL (Jiang et al. 2013, Zhou et al. 2013). Despite the crucial role of D3 in the AM fungal colonization process, the *d14* mutant is colonized at even higher levels than WT plants (Yoshida et al. 2012). Recently, it has been shown that D14-LIKE (D14L) is required for AM fungal colonization (Gutjahr et al. 2015a). Rice D14L is a receptor for karrikin, a plant growth regulator first identified in smoke (Flematti et al. 2004), which belongs to a different evolutionary clade from D14. Since D14L is not thought to be involved in SL signaling in rice (Arite et al. 2009, Hu et al. 2010, Kameoka and Kyozuka, 2015, Gutjahr et al. 2015a), it is not yet clear whether SLs are involved not only in pre-symbiotic chemical dialogs but also in the root colonization step. Importantly, there are also studies that indicate a tight link between the synthesis of carotenoid derivatives and root colonization (Fester et al. 2002, Floss et al. 2008a, Sun et al. 2008, Vogel et al. 2010). Therefore, the influence of SL biosynthesis on AM fungal colonization should be investigated not only in terms of typical SL signaling but also from a wider perspective.

The cause of the inhibition of AM colonization in SL-deficient mutants has not been clarified (Waters et al. 2017). AM are developed by the successive formation of infection units (IUs) that are composed of an internal mycelium arising from entry points (Cox and Sanders 1974, Sanders and Sheikh 1983, Walker and Smith 1984, Kobae et al. 2016). In addition, IUs are ephemeral structures with a lifetime at maturity of within <3 d in rice seedlings (Kobae and Fujiwara 2014). Thus, when one of the elements that support the successive formation of IUs is lost, its effect has a major impact on the entire mycorrhization in a short time (Kobae et al. 2016). Therefore, in order to investigate the role of SLs in colonization processes accurately, it is important to focus on the analysis of the development of each IU with high spatiotemporal resolution. In the present study, detailed morphological analysis of AM fungal colonization processes, including hyphopodium formation, hyphal entry into the roots and intraradical colonization, was performed in SL biosynthesis mutants of rice. Our data reveal the crucial roles of SL biosynthesis genes in the punctual hyphal entry of AM fungi into roots and in the maintenance of subsequent successive colonization.

Results

Expression of SL biosynthesis genes is partly up-regulated in colonized roots

We first tested whether the expression of SL biosynthesis genes is up-regulated in accordance with AM fungal colonization. We performed RNA sequencing (RNA-seq) analysis to monitor the transcriptional changes in the SL biosynthesis pathway in rice roots colonized with the model fungus *R. irregularis* DAOM197198 at 15 days post-planting (d.p.p.). Some genes responsible for SL biosynthesis (e.g. *D27*, *D17*, *D10* and *MAX1*) and the homologous genes for SL signaling modules [e.g. *D14-like2* genes (*D14L2* genes) and *D53-like*] responded to the inoculation of *R. irregularis* (**Supplementary Table S1**), suggesting the up-regulation of the SL biosynthesis pathway in the early stages of AM colonization. Quantitative reverse transcription–PCR (RT–PCR) analyses revealed that the transcript levels of symbiotic phosphate transporter 11 (*PT11*) (Paszkowski et al. 2002, Kobae and Hata 2010) and *D27* relative

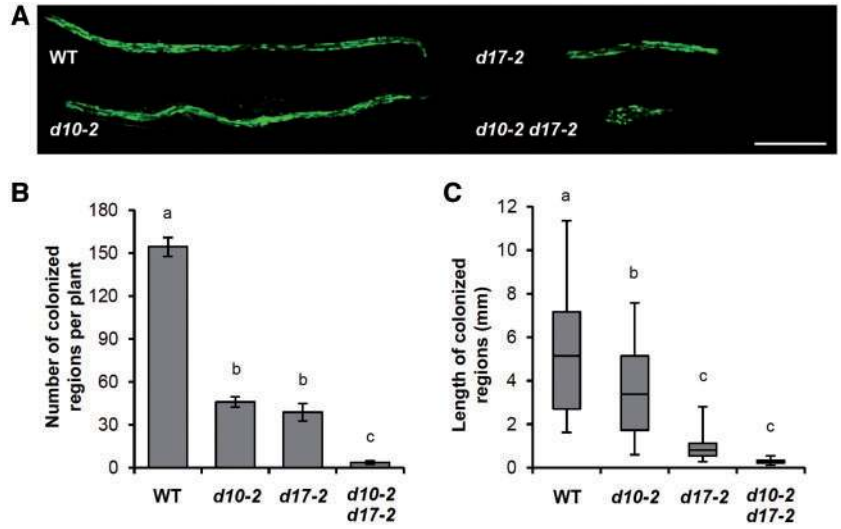

Fig. 1 Longitudinal extension of colonized regions is reduced in *d10-2* and *d17-2* mutants. (A) Cell wall staining of *Rhizophagus irregularis* colonizing roots of the WT and SL-deficient mutants of rice (25 d.p.p.). The fungal cell wall was detected with FITC-conjugated WGA. (B) The number of colonized regions per plant (25 d.p.p.). Data are given as means ± SD ($n = 3$). (C) The longitudinal length of each colonized region (25 d.p.p.). The lengths of 12–30 colonized regions from three plants (25 d.p.p.) were measured using ImageJ. The middle lines of box plots represent median values, with bars showing value ranges (minimum to maximum). Different letters indicate significant differences as assessed by Tukey's HSD test ($P < 0.05$). Scale bar = 1 mm.

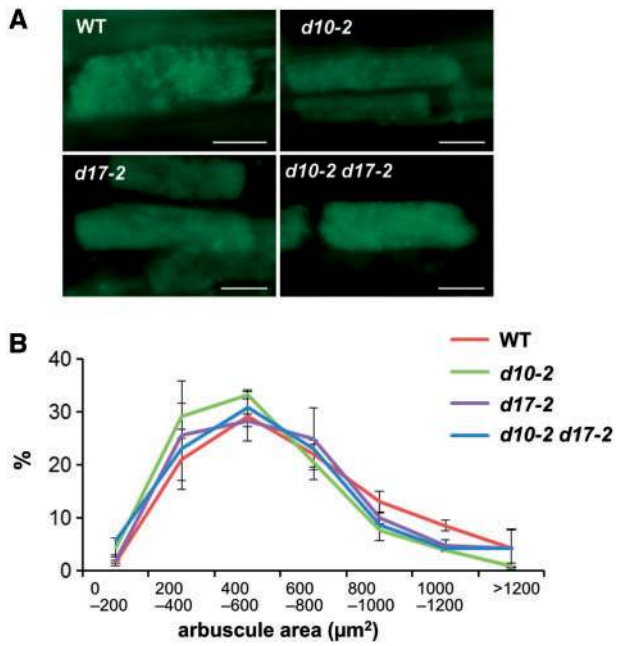

Fig. 2 Arbuscule formation is normal in SL-deficient mutants. (A) WGA–FITC staining of arbuscules (*Rhizophagus irregularis*) in the roots of the WT and SL-deficient mutants of rice (25 d.p.p.). (B) Arbuscule size distribution. The areas of longitudinal optical sections of arbuscules (250 arbuscules from each plant of the WT, *d10-2* and *d17-2*) were measured. Data are given as means ± SD ($n = 3$). The size distribution of a total of 139 arbuscules from three *d10-2 d17-2* plants is also shown. Scale bar = 20 μm.

to those of the rice *CYCLOPHILIN2* gene (Gutjahr et al. 2008) were significantly elevated in colonized roots in comparison with non-colonized roots (**Supplementary Fig. S1**). The transcript levels of *D17*, *D10* and *Max1* (*Os900*) in colonized roots also showed signs of fluctuation; however, they were not statistically significant differences (**Supplementary Fig. S1**).

Development of colonized regions is suppressed in *d10-2* and *d17-2* mutants

To investigate whether SL biosynthesis genes are required for the intraradical colonization of AM fungi, WT and SL-deficient mutants, *d10-2* (Umehara et al. 2008), *d17-2* and *d10-2 d17-2* double mutants of rice (all Nipponbare background), were inoculated with *R. irregularis*, and the roots were subjected to fungal cell wall staining with fluorescein isothiocyanate (FITC)-conjugated wheat germ agglutinin (WGA) at 25 d.p.p. (**Fig. 1A**). Compared with the WT, the number of colonized regions per plant was significantly decreased in *d10-2*, *d17-2* and *d10-2 d17-2* mutants (**Fig. 1B**). The term 'colonized region' was used in reference to hyphal-colonized root regions, and single colonized regions were bound by two infection fronts comprising intercellular hyphae (Buwalda et al. 1984, Kobae et al. 2016). Although the number of colonized regions was similar between *d10-2* and *d17-2* mutants, the number of colonized regions in *d10-2 d17-2* double mutants was significantly more suppressed (**Fig. 1B**). Moreover, the longitudinal length of colonized regions in *d17-2* was significantly shorter than that in *d10-2*, and the reduction was also additively observed in *d10-2 d17-2* double mutants (**Fig. 1C**). However, arbuscule sizes in these mutants, as indicated by FITC–WGA staining, were comparable with those in the WT (**Fig. 2**). Reduced extension of colonized regions was also observed in *d10-1* and *d17-1* mutants of the Shiokari background (**Supplementary Fig. S3**). The shoot branching phenotype and the ratio of the root types (crown roots, large lateral roots and fine lateral roots) (Gutjahr et al. 2009) between the WT and SL-deficient mutants showed differences, but

there were no significant differences among the SL-deficient mutants tested (**Supplementary Fig. S2**).

Infection unit development is not suppressed in SL-deficient mutants

To determine the colonization step that leads to reduced growth of colonized regions, we performed detailed morphological analysis of AM fungi in the roots of SL-deficient mutants. According to the observations of mycorrhization processes in early studies (Sanders and Sheikh 1983, Bonfante-Fasolo 1984, Buwalda et al. 1984) and recent live imaging of rice mycorrhizal roots (Kobae and Fujiwara 2014), it was expected that colonization processes as described below would be observed in WT roots (**Supplementary Fig. S4**). After the formation of the initial IU, in many cases subsequent IU formation occurs immediately adjacent to the established IU through external hypha connecting these IUs. Each IU has a short life span; accordingly, 'successive formation' of IUs underlies the development of colonized regions. To monitor the morphological changes in the colonization process of AM fungi in SL-deficient mutants, we performed temporal observation of the longitudinal length of colonized regions, hyphopodium number and arbuscule number (**Supplementary Fig. S5**). The length of colonized regions in WT roots was drastically increased at 14 and 15 d.p.p., whereas that in *d10-2* and *d17-2* mutants was slowly increased by up to 18 d.p.p. (**Fig. 3A**). Intraradical colonization was not observed in *d10-2 d17-2* double mutants by up to 15 d.p.p. The number of hyphopodia per colonized region in WT roots was also drastically increased at 14 and 15 d.p.p., whereas that in *d10-2* and *d17-2* was not drastically increased up to 18 d.p.p. (**Fig. 3B**). Remarkably, the number of arbuscules per hyphopodium did not decrease in SL-deficient mutants (**Fig. 3C**). Lengths of colonized regions per hyphopodium (i.e. mean length of an IU) were also maintained in SL-deficient mutants (**Fig. 3D**). The data suggested that the frequency of IU formation was decreased. To assess the possibility that reduced SL biosynthesis could not boost the metabolic activity of the intraradical mycelium to maintain successive colonization at the early colonization stages, colonization levels were analyzed by vital staining of AM fungi from 11 to 14 d.p.p. Vital staining with nitro-blue tetrazolium (NBT) detects in situ succinate dehydrogenase (SDH) activity of AM fungus as a blue precipitation (MacDonald and Lewis 1978, Kobae et al. 2014). The numbers of colonized regions were drastically increased in the WT up to 14 d.p.p., whereas the numbers were not increased in *d10-2* and *d17-2* mutants (**Fig.4A**). Double histochemical staining of metabolic activities and the cell wall of the intraradical mycelium (**Supplementary Fig. S6**) revealed that all intraradical colonization in WT, *d10-2* and *d17-2* roots had metabolic activities, suggesting that vital staining successfully detected all the colonized regions. Remarkably, the length of colonized regions evaluated by vital staining in *d10-2* and *d17-2* mutants was comparable with that in the WT at 12–14 d.p.p. (**Fig. 4B**). These observations suggested that the metabolic activities and development of IUs were not suppressed in SL-deficient mutants, once the colonizations are initiated.

Hyphal entry of AM fungus into roots is severely attenuated in SL-deficient mutants

To determine which colonization step leads to the attenuation of successive colonization in SL-deficient mutants, the morphology of AM hyphae at the earliest colonization stages was investigated. During the pre-symbiotic stage, the hyphae clung to roots and showed several orders of branching around roots. We called the hyphal branching in at least three orders around roots 'rhizospheric hyphal branching' (**Supplementary Figs. S7**, **S8**). In WT roots, this branching was observed at 7 d.p.p. and the number of rhizospheric hyphal branches (RHBs) observed increased up to 11 d.p.p. (**Fig. 5A**). Colonized regions were not observed at 7 d.p.p.; however, the numbers of colonized regions observed drastically increased at 10 and 11 d.p.p. in the WT (**Fig. 5B**). Remarkably, in WT roots, approximately 70% of RHBs developed a hyphopodium, which penetrated the root epidermis from 8 to 11 d.p.p. (**Fig. 5C; Supplementary Fig. S9**), suggesting the prompt occurrence of epidermal penetration during rhizospheric hyphal branching. In *d10-2* and *d17-2* mutants, the first observation of RHBs was delayed by at least 1 d compared with that in the WT; however, the numbers of RHBs observed from 8 to 11 d.p.p. were comparable with those of the WT from 7 to 10 d.p.p. (**Fig. 5A**). Colonized regions in *d10-2* and *d17-2* were hardly observed up to 11 d.p.p. (**Fig. 5B**), suggesting a delay in hyphal entry into roots. In addition to the prompt epidermal penetration in WT roots, hyphopodium formation was significantly attenuated in *d10-2* and *d17-2* up to 11 d.p.p. (**Fig. 5C**). Hyphopodia formed in *d10-2* and *d17-2* roots were morphologically normal, and septate hyphopodial hyphae reported in some symbiotic signaling mutants (Yoshida et al. 2012, Nadal et al. 2017) were not observed (**Supplementary Fig. S9**). In SL-deficient mutants, the hyphopodium penetrated the intercellular spaces of the epidermis, penetrated further into the hypodermal cells and formed coiled hyphae (**Supplementary Fig. S10**). Such a colonization pattern was the same as in the WT, suggesting that SL biosynthesis genes are not required for hyphal penetration into the roots but for efficient hyphopodium formation leading to punctual intraradical colonization.

Discussion

SL biosynthesis genes are required for punctual hyphal entry into roots

Time course observations of AM hyphal morphology in roots during the early mycorrhization stages (7–18 d.p.p.) revealed that hyphopodium formation was severely attenuated, whereas subsequent growth of IUs was not suppressed in SL-deficient mutants. However, the growth of colonized regions was severely suppressed in SL-deficient mutants at a later mycorrhization stage (25 d.p.p.). Given that colonized regions develop through the successive formation of IUs that develop immediately adjacent to an established IU (Sanders and Sheikh 1983, Kobae et al. 2016), the reduction in the growth of colonized regions in SL-deficient mutants is probably due to reduced

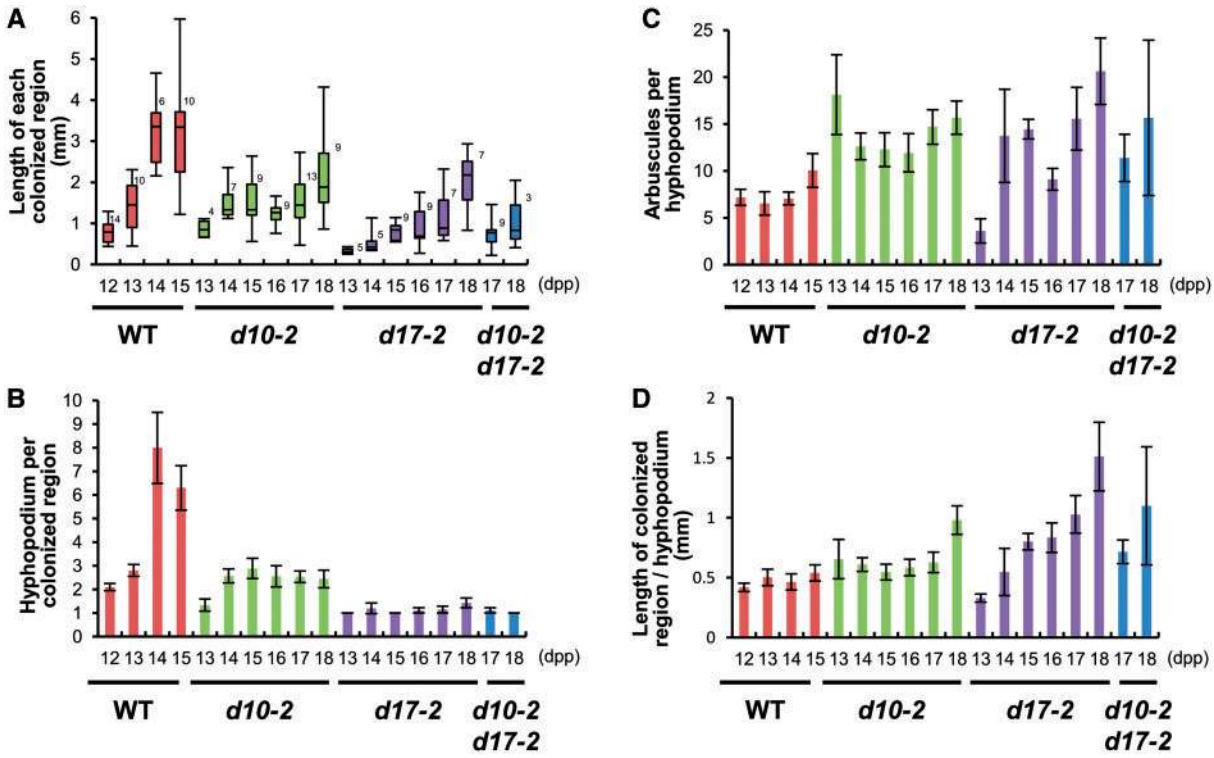

Fig. 3 Growth of the infection unit is not suppressed in SL-deficient mutants. Roots of the WT and SL-deficient mutants colonized with *Rhizophagus irregularis* were stained with WGA–FITC at 12–15 d.p.p. for the WT, 13–18 d.p.p. for the *d10-2* and *d17-2* mutants, and 17 and 18 d.p.p. for the *d10-2 d17-2* mutant. (A) The length of each colonized region. Colonized regions were randomly selected from three plants of each line and values above the boxes indicate the numbers of colonized regions analyzed. The middle lines of box plots represent median values, with bars showing value ranges (minimum to maximum). (B) Hyphopodium number per colonized region. (C) Arbuscule number per hyphopodium. (D) Length of colonized region per hyphopodium. Data are given as means ± SE (B–D). No intraradical colonization was observed at 12 d.p.p. in *d10-2* and *d17-2* mutants, and at 12–16 d.p.p. in the *d10-2 d10-7* mutant.

hyphal entry into roots. Our observations indicate a novel role for SL biosynthesis genes in the development of mycorrhizal roots: SL biosynthesis genes are required for the efficient formation of a hyphopodium, leading to the hyphal entry into roots, which substantially influences the subsequent development of colonization (**Fig. 6**).

The mechanisms underlying the control of hyphal entry by SL biosynthesis genes are unknown. Conceptually, increased production of SLs accompanying the approach of AM fungi forms a sharp concentration gradient of SLs around the root, which may be positional information for the root surface (Nadal and Paszkowski, 2013) that is necessary for rapid infection of AM fungi. An elevated concentration of SLs in close proximity to roots may be necessary to exceed a threshold to initiate hyphopodium formation. To date, different studies have obtained different results as to whether SL biosynthesis is up-regulated in mycorrhizal roots relative to non-mycorrhizal roots (Floss et al. 2008b, Sun et al. 2008, Gomez et al. 2009, Guether et al. 2009, Hogekamp et al. 2011, López-Ráez et al. 2011, Gaude et al. 2012, Hogekamp and Küster 2013, Handa et al. 2015, Gutjahr et al. 2015b). *CCD7* transcripts in the monoxenic cultures of *R. irregularis* with tomato roots have been shown to be up-regulated before intraradical colonization (López-Ráez et al. 2015). The expression of SL biosynthesis genes is regulated by two GRAS transcription factors, NSP1 and NSP2 (Liu et al. 2011, Delaux et al. 2013, Takeda et al. 2013), and SL levels in roots and AM colonization are decreased in the *nsp1 nsp2* double mutant in both *Medicago truncatula* and rice (Liu et al. 2011). A recent study has shown that tomato *Sl-IAA27*, which is an auxin signaling-related gene and is required for mycorrhization, regulates the expression of *NSP1*, *MAX1* and *D27* (Guillotin et al. 2016). The expression of *Sl-IAA27* is induced by the fungus before any root–fungus physical contact, suggesting the presence of diffusible fungal signals that trigger SL biosynthesis in roots (Guillotin et al. 2016). In *M. truncatula*, *D27* transcript accumulation is slightly increased after Myc-lipo-chito-oligosaccharide (Myc-LCO) treatment (Hohnjec et al. 2015). However, the expression of *CCD7* is not strongly induced by the treatment of short-chain COs (Giovannetti et al. 2015) or Myc-LCOs (Camps et al. 2015), suggesting that the up-regulation of SL biosynthesis is driven by a mixture of fungal COs and Myc-LCOs (Sun et al. 2015) or additional chemicals (Bonfante and Requena, 2011, Nadal and Paszkowski 2013, Schmitz and Harrison 2014). Alternatively, the up-regulation of SL biosynthesis may be driven by the perception of a high concentration of fungal signals (Nadal and Paszkowski 2013, Schmitz and Harrison 2014), which is probably achieved by the close contact of two symbionts. In this

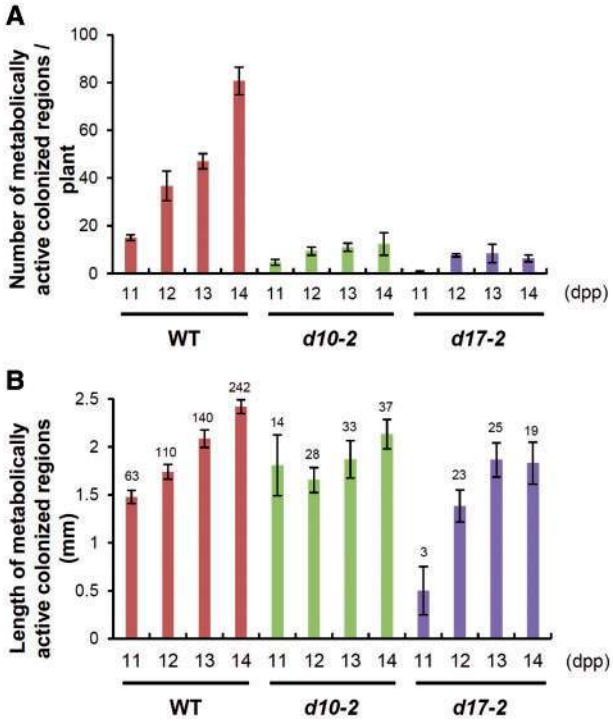

Fig. 4 Intraradical colonization is metabolically active in SL-deficient mutants. Roots of the WT and SL-deficient mutants colonized with *Rhizophagus irregularis*. Colonized regions were detected by vital staining at 11, 12, 13 and 14 d.p.p. (A) The number of colonized regions per plant. Three plants were analyzed. (B) Length of colonized regions. The length of all colonized regions of (A) was measured. Values above columns indicate the numbers of colonized regions analyzed. Data are given as means ± SE.

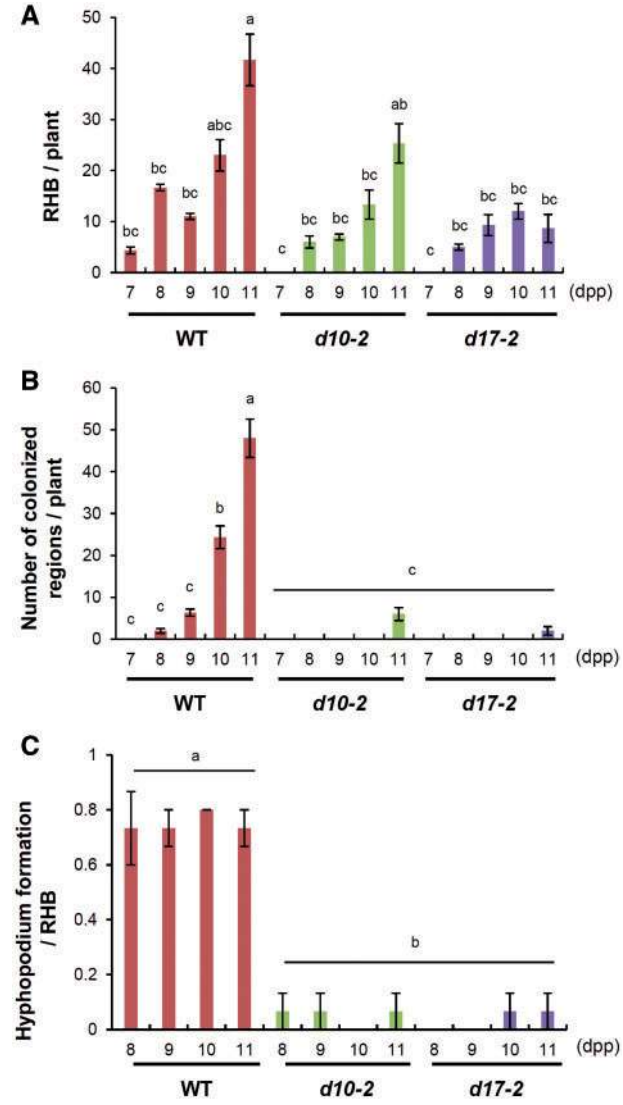

Fig. 5 Hyphopodium formation is attenuated in SL-deficient mutants. Roots of the WT and SL-deficient mutants colonized with *Rhizophagus irregularis* were stained with WGA–HRP–DAB at 7–11 d.p.p. Three plants were analyzed. (A) The number of rhizopheric hyphal branches (RHBs) per plant. (B) The number of colonized regions per plant. (C) Hyphopodium formation per RHB. Numbers of hyphopodia in five randomly chosen RHBs were measured. Data are given as means ± SE. Different letters indicate significant differences as assessed by Tukey's HSD test ($P < 0.05$).

study, we showed that only the *D27* transcript increased in mycorrhizal roots. Remarkably, the expression of *Sl-IAA27* is positively regulated by the presence of AM fungi, but negatively regulated in the immediate vicinity of intraradical AM fungal structures (Guillotin et al. 2016). In future research, it will be necessary to investigate further the relationship between regulation of transcription levels of SL biosynthesis genes and the colonization process with higher temporal and spatial resolution.

Different roles of D10 and D17 in mycorrhizal roots

SLs are not detected in the shoots, roots and root exudates of all rice SL-deficient mutants (e.g. *d27*, *d10* and *d17*) by LC-MS/MS quantification (Umehara et al. 2008, Lin et al. 2009). Nevertheless, AM colonization levels between *d10* and *d17* mutants are significantly different, and the additive phenotype is observed in *d10-2 d17-2* double mutants, while the difference in the shoot and root branching phenotype is not apparent. There are two possible explanations for this. First, there may be residual amounts of SLs in the *d10-2* and *d17-2* mutants with an uncharacterized mechanism. In this case, the *d10-2 d17-2* double mutants may further reduce the SL amounts and therefore show the more severe phenotype. Secondly, there may be a distinct role for D17 in the development of intraradical colonization. In the plant apocarotenoid synthesis pathway, D17/CCD7 catalyzes C_{40} carotenoid precursors to provide resultant C_{27} precursors not only to D10/CCD8 for C_{18} apocarotenoid and SL formation but also to CCD1 for the synthesis of AM-induced C_{14} apocarotenoids with a yellow pigment (Walter et al. 2015), called mycorradicin (Klingner et al. 1994, Maier et al. 1995). Although *M. truncatula* in which *CCD1* is knocked down can form normal mycorrhizal roots (Floss et al. 2008b), tomato *CCD1a* is clearly induced in arbuscule-containing cells at later stages of colonization (8-week-old tomato roots) but not in the roots at pre-symbiotic stages (up to 4 d post-inoculation) (López-Ráez et al. 2015). The authors proposed that

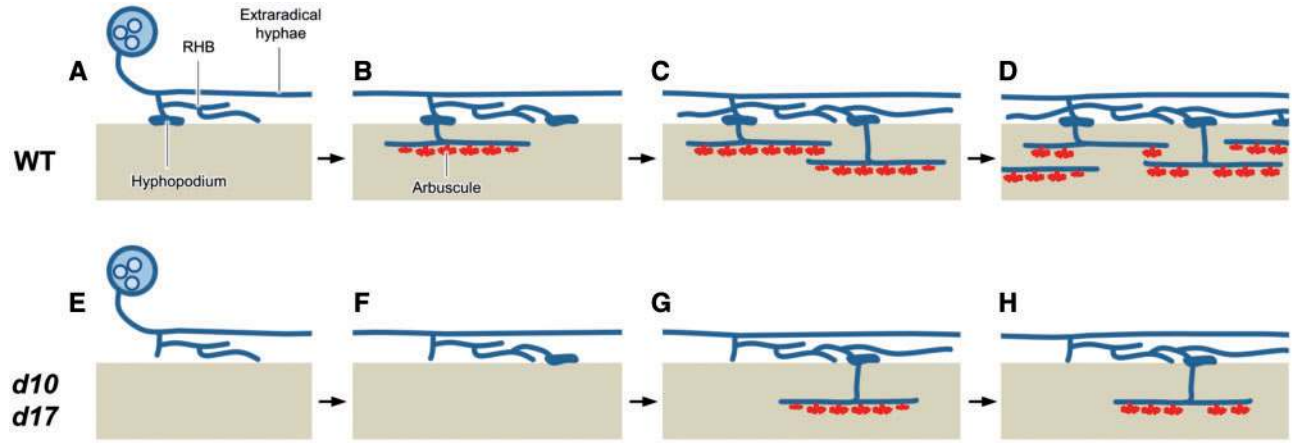

Fig. 6 Model diagram of the phenotype of SL-deficient mutants. In the WT, the occurrence of rhizospheric hyphal branching is immediately followed by the formation of hyphopodia on roots (A). Successive formation of infection units (B, C) contributes to the rapid expansion of colonized regions (D). In SL-deficient mutants, RHB formation is delayed by 1 d and is not accompanied by the formation of hyphopodia (E). Hyphopodium formation and intraradical colonization are severely delayed (F), but the development and the metabolic activity of infection units are nor suppressed (G). Due to the attenuated hyphopodium formation, the development of colonized regions is severely inhibited (H).

mycorradicin may be important for the later stages of mycorrhization and particularly for the maintenance of arbuscules (López-Ráez et al. 2015). Consistent with this, we showed that the timing of RHB formation and the number of hyphopodia were not significantly different between *d10* and *d17* mutants up to 11 d.p.p., whereas the length of colonized regions of *d17-2* at 25 d.p.p. was significantly reduced in comparison with that of *d10-2*, suggesting the distinct role of D17 in the development of intraradical colonization. However, it should be noted that AM colonization proceeds through the successive formation of IUs (Sanders and Sheikh 1983, Kobae et al. 2016); thus, a short delay in epidermal penetration that cannot be easily detected may also lead to the reduction of the colonization level at the later stages of mycorrhization. Further analysis will be required to clarify the functional relationship between D17, D10 and CCD1.

In this study, we show that AM fungal hyphae are able to come close to roots even in the absence of *D17* and *D10* genes which are required for major SL biosynthesis; however, *D17* and *D10* play a crucial role in facilitating the entry of AM fungal hyphae into roots. We tested only one concentration of spores (500 spores per pot), which may be too high to conclude that hyphae normally come closer to mutant roots relative to WT roots. However, compared with the WT, hyphopodium formation and intraradical colonization in SL-deficient mutants after RHB formation were significantly delayed, indicating that SL biosynthesis genes control hyphal entry into roots. Our previous observations of AM development suggest that IUs are ephemeral structures with a lifetime at maturity of within <3 d in rice (Kobae and Hata 2010); accordingly, mycorrhization proceeds through the successive formation of IUs (Sanders and Sheikh 1983, Kobae et al. 2016). This indicates that the regulation of SL biosynthesis genes potentially effectively controls the colonization level of AM fungi. In future studies, it will be intriguing to clarify the role of the SL synthesis pathway in controlling the level of AM fungal colonization by investigating in detail how SL biosynthesis genes are regulated depending on plant nutrition, environmental conditions and the type of AM fungi.

Materials and Methods

Plant materials

Rice (*Oryza sativa* L. cv. Nipponbare) WT, *d17-2*, *d10-2* (Umerara et al. 2008, Minakuchi et al. 2010) and *d17-2 d10-2* double mutant were used as plant materials. The *d17-2* mutant was isolated from a population of tissue culture-derived plants. PCR amplification and sequencing of *D17* genomic regions in *d17-2* revealed a deletion of 36 nucleotides at the first intron and second exon junction (**Supplementary Fig. S11**). The *d17-2 d10-2* double mutant was generated by crossing the *d17-2* and *d10-2* mutant.

Plant growth, fungal material and inoculation

Seeds were surface sterilized with bleach (2.5% available chloride) for 5 min, rinsed with excess deionized water five times and immersed in deionized water for 2 d at 28°C. The germinated seeds were grown in 100 ml polypropylene pots. The soil consists of 20 g (bottom layer) of Akadama soil (tuff loam) (Setogahara Kaen) and 45 g (upper layer) of a Kanuma soil (weathered volcanic lapillus)/Ezo sand (small pumice)/Nippi soil (granular potting soil with nutrients) (Nihon Hiryo) mixture (6 : 2 : 1, by weight). Plants were inoculated with *R. irregularis* DAOM197198 (Premier Tech) by mixing 500 spores throughout the upper soil mixture before planting the germinated seeds. Plant pots were placed in a flat-bottomed tray in a growth chamber under 15 h light/9 h dark photoperiods (26–30/23–25°C). Water was supplied from the bottom by maintaining a water level up to 5 mm in depth.

Total RNA extraction and quantitative RT–PCR

Total RNA was extracted from mycorrhizal or non-mycorrhizal roots using an RNeasy Plant Mini kit (Qiagen) according to the manufacturer's instructions. The yield and purity of the RNA were determined spectrophotometrically (NanoDrop, Thermo Fisher Scientific). First-strand cDNA was synthesized from 800–1,400 ng of total RNA prepared from whole roots and root fragments using a High Capacity RNA to cDNA Kit (Thermo Fisher Scientific) according to the manufacturer's instructions. Specific cDNAs were amplified by SYBR Premix Ex Taq II (TAKARA) and gene-specific primers (**Supplementary Table S2**) using real-time PCR (QuantStudio 3, Thermo Fisher Scientific). PCRs were 94°C for 2 min and 40 cycles of 94°C for 15 s, 56°C for 30 s and 72°C for 30 s. The specificity of each PCR product was assessed with the dissociation curve

(94°C for 15 s, 60°C for 1 mi, and 94°C for 1 s). The transcript levels of the target gene were calculated by the relative standard curve method using the *CYCLOPHILIN2* gene as internal standard.

Fungal cell wall staining

AM fungal structures in roots were detected by FITC–WGA or 3,3′-diaminobenzidine (DAB) staining with horseradish peroxidase (HRP)–WGA as described previously (Kobae and Fujiwara 2014, Kobae and Ohtomo 2016).

Fungal vital staining

To detect metabolically active AM fungal colonization in roots, the viability was assessed by vital staining, which detects in situ SDH activity using NBT (MacDonald and Lewis 1978). Washed roots were incubated at room temperature for 30 min in the dark in NBT solution containing 50 mM Tris–HCl buffer (pH 7.4), 1 mg ml^{-1} NBT, 0.5 mM $MgCl_2$ and 250 mM sodium succinate, and then rinsed with water. Images were obtained using a stereomicroscope equipped with a CCD camera

Microscopy

Colonized sites were located and dissected using a fluorescence stereomicroscope (Leica M165FC) and then analyzed using an epi-fluorescence microscope (Zeiss Axio observer. A1) equipped with a green fluorescent protein (GFP) long pass filter (FS16: BP485/20, FT510, LP515). The lengths of colonized regions and the sizes of arbuscules were measured using ImageJ (http://rsb.info.nih.gov/ij/index.html).

RNA-seq analysis

Two biological replicates were prepared for RNA-seq experiments. Total RNA was extracted from the mycorrhizal or non-mycorrhizal roots using an RNeasy Plant Mini kit (Qiagen). Genome DNA was removed from the RNA solution by digesting with RNase-free DNase (Qiagen). The quality of total RNA was assessed on an Agilent 2100 Bioanalyzer (Agilent Technologies). Sequencing libraries were constructed using the TruSeq RNA Sample Prep kit (Illumina) according to the manufacturer's instructions. Paired-end sequencing (2×100 bp) was performed by Illumina HiSeq 2000. The genomic sequence of *O. sativa* was obtained from the MSU Rice Genome Annotation Project Release 7 (http://rice.plantbiology.msu.edu/) (Kawahara et al. 2013). Raw sequence reads were mapped against the *O. sativa* genomic sequence by TopHat software (Trapnell et al. 2009). The mapped reads were counted for annotated genes using intersectBed in the BEDTools package (Quinlan and Hall 2010). The read counts were normalized with the iDEGES/edgeR method (Sun et al. 2013). Genes differentially expressed between the mycorrhizal and non-mycorrhizal roots were detected by edgeR (Robinson et al. 2010) at a false discovery rate cut-off of 0.001. Data sets of the short reads were deposited in the DDBJ Sequence Read Archive (accession No. SSUB006029).

Supplementary Data

Supplementary data are available at PCP online.

Funding

This work was supported by the Ministry of Education, Culture, Sports, Science and Technology of Japan [Grants-in-Aid from the NC-CARP project, Grant-in-Aid for Scientific Research on the Innovative Areas (grant No. JP22128006)] and by the Japan Science and Technology Agency [ACCEL grant No. JPMJAC1403].

Acknowledgments

We thank Shigo Hata for useful discussion, and Hiroshi Moriyama (Nihon Hiryo Co. Ltd.) for providing Nippi soil.

Disclosures

The authors have no conflicts of interest to declare.

References

Akiyama, K., Matsuzaki, K. and Hayashi, H. (2005) Plant sesquiterpenes induce hyphal branching in arbuscular mycorrhizal fungi. *Nature* 435: 824–827.

Alder, A., Jamil, M., Marzorati, M., Bruno, M., Vermathen, M., Bigler, P., et al. (2012) The path from β-carotene to carlactone, a strigolactone-like plant hormone. *Science* 335: 1348–1351.

Arite, T., Umehara, M., Ishikawa, S., Hanada, A., Maekawa, M., Yamaguchi, S., et al. (2009) *d14*, a strigolactone-insensitive mutant of rice, shows an accelerated outgrowth of tillers. *Plant Cell Physiol.* 50: 1416–1424.

Bécard, G. and Fortin, J.A. (1988) Early events of vesicular-arbuscular mycorrhiza formation on Ri T-DNA transformed roots. *New Phytol.* 108: 211–218.

Besserer, A., Bécard, G., Jauneau, A., Roux, C. and Séjalon-Delmas, N. (2008) GR24, a synthetic analog of strigolactones, stimulates the mitosis and growth of the arbuscular mycorrhizal fungus *Gigaspora rosea* by boosting its energy metabolism. *Plant Physiol.* 148: 402–413.

Besserer, A., Puech-Pagès, V., Kiefer, P., Gomez-Roldan, V., Jauneau, A., Roy, S., et al. (2006) Strigolactones stimulate arbuscular mycorrhizal fungi by activating mitochondria. *PLoS Biol.* 4: e226.

Bonfante-Fasolo P. (1984) Anatomy and morphology of VA mycorrhizae. *In* VA Mycorrhizas. Edited by Powell, C.L. and Bagyaraj, D.J. pp. 5–33. CRC Press, Boca Raton, FL.

Bonfante, P. and Genre, A. (2010) Mechanisms underlying beneficial plant–fungus interactions in mycorrhizal symbiosis. *Nat. Commun.* 1: 48.

Bonfante, P. and Requena, N. (2011) Dating in the dark: how roots respond to fungal signals to establish arbuscular mycorrhizal symbiosis. *Curr Opin. Plant Biol.* 14: 451–457.

Borghi, L., Liu, G.W., Emonet, A., Kretzschmar, T. and Martinoia, E. (2016) The importance of strigolactone transport regulation for symbiotic signaling and shoot branching. *Planta* 243: 1351–1360.

Buee, M., Rossignol, M., Jauneau, A., Ranjeva, R. and Bécard, G. (2000) The presymbiotic growth of arbuscular mycorrhizal fungi is induced by a branching factor partially purified from plant root exudates. *Mol. Plant Microbe. Interact.* 13: 693–698.

Buwalda, J.G., Stribley, D.P. and Tinker, P.B. (1984) The development of endomycorrhizal root systems. V. The detailed pattern of development of infection and the control of infection level by host in young leek plants. *New Phytol.* 96: 411–427.

Camps, C., Jardinaud, M.F., Rengel, D., Carrère, S., Hervé, C., Debellé, F., et al. (2015) Combined genetic and transcriptomic analysis reveals three major signalling pathways activated by Myc-LCOs in *Medicago truncatula*. *New Phytol.* 208: 224–240.

Cardoso, C., Zhang, Y., Jamil, M., Hepworth, J., Charnikhova, T., Dimkpa, S.O., et al. (2014) Natural variation of rice strigolactone biosynthesis is associated with the deletion of two MAX1 orthologs. *Proc. Natl. Acad. Sci. USA* 111: 2379–2384.

Cook, C.E., Whichard, L.P., Turner, B., Wall, M.E. and Egley, G.H. (1966) Germination of witchweed (*Striga lutea* Lour.): isolation and properties of a potent stimulant. *Science* 154: 1189–1190.

Courty, P.E., Smith, P., Koegel, S., Redecker, D. and Wipf, D. (2015) Inorganic nitrogen uptake and transport in beneficial plant root–microbe interactions. *Crit. Rev. Plant Sci.* 34: 4–16.

Cox, G. and Sanders, F. (1974) Ultrastructure of the host–fungus interface in a vesicular-arbuscular mycorrhiza. *New Phytol.* 73: 901–912.

Delaux, P.M., Bécard, G. and Combier, J.P. (2013) NSP1 is a component of the Myc signaling pathway. *New Phytol.* 199: 59–65.

Fester, T., Hause, B., Schmidt, D., Halfmann, K., Schmidt, J., Wray, V., Hause, G. and Strack, D. (2002) Occurrence and localization of apocarotenoids in arbuscular mycorrhizal plant roots. *Plant Cell Physiol.* 43: 256–265.

Flematti, G.R., Ghisalberti, E.L., Dixon, K.W. and Trengove, R.D. (2004) A compound from smoke that promotes seed germination. *Science* 305: 977.

Floss, D.S., Hause, B., Lange, P.R., Kuster, H., Strack, D. and Walter, M.H. (2008a) Knock-down of the MEP pathway isogene 1-deoxy-D-xylulose 5-phosphate synthase 2 inhibits formation of arbuscular mycorrhiza-induced apocarotenoids, and abolishes normal expression of mycorrhiza-specific plant marker genes. *Plant J.* 56: 86–100.

Floss, D.S., Schliemann, W., Schmidt, J., Strack, D. and Walter, M.H. (2008b) RNA interference-mediated repression of *MtCCD1* in mycorrhizal roots of *Medicago truncatula* causes accumulation of C27 apocarotenoids, shedding light on the functional role of CCD1. *Plant Physiol.* 148: 1267–1282.

Foo, E., Yoneyama, K., Hugill, C.J., Quittenden, L.J. and Reid, J.B. (2013) Strigolactones and the regulation of pea symbioses in response to nitrate and phosphate deficiency. *Mol. Plant* 6: 76–87.

Gaude, N., Bortfeld, S., Duensing, N., Lohse, M. and Krajinski, F. (2012) Arbuscule-containing and non-colonized cortical cells of mycorrhizal roots undergo extensive and specific reprogramming during arbuscular mycorrhizal development. *Plant J.* 69: 510–528.

Genre, A., Chabaud, M., Balzergue, C., Puech-Pagès, V., Novero, M., Rey, T., et al. (2013) Shortchain chitin oligomers from arbuscular mycorrhizal fungi trigger nuclear Ca^{2+} spiking in *Medicago truncatula* roots and their production is enhanced by strigolactone. *New Phytol.* 198: 190–202.

Giovannetti, M., Mari, A., Novero, M. and Bonfante, P. (2015) Early *Lotus japonicus* root transcriptomic responses to symbiotic and pathogenic fungal exudates. *Front. Plant Sci.* 6: 480.

Giovannetti, M., Sbrana, C. and Logi, C. (1994) Early process involved in host recognition by arbuscular mycorrhizal fungi. *New Phytol.* 127: 703–709.

Gomez, S.K., Javot, H., Deewatthanawong, P., Torres-Jerez, I., Tang, Y., Blancaflor, E.B., et al. (2009) *Medicago truncatula* and *Glomus intraradices* gene expression in cortical cells harboring arbuscules in the arbuscular mycorrhizal symbiosis. *BMC Plant Biol.* 9: 10.

Gomez-Roldan, V., Fermas, S., Brewer, P.B., Puech-Pagès, V., Dun, E.A., Pillot, J.P., et al. (2008) Strigolactone inhibition of shoot branching. *Nature* 455: 189–194.

Guether, M., Balestrini, R., Hannah, M., He, J., Udvardi, M.K. and Bonfante, P. (2009) Genome-wide reprogramming of regulatory networks, transport, cell wall and membrane biogenesis during arbuscular mycorrhizal symbiosis in *Lotus japonicus*. *New Phytol.* 182: 200–212.

Guillotin, B., Etemadi, M., Audran, C., Bouzayen, M., Bécard, G. and Combier, J.P. (2016) *Sl-IAA27* regulates strigolactone biosynthesis and mycorrhization in tomato (var. MicroTom). *New Phytol.* 213: 1124–1132.

Gutjahr, C., Banba, M., Croset, V., An, K., Miyao, A., An, G., et al. (2008) Arbuscular mycorrhiza-specific signaling in rice transcends the common symbiosis signaling pathway. *Plant Cell* 20: 2989–3005.

Gutjahr, C., Casieri, L. and Paszkowski, U. (2009) *Glomus intraradices* induces changes in root system architecture of rice independently of common symbiosis signaling. *New Phytol.* 182: 829–837.

Gutjahr, C., Gobbato, E., Choi, J., Riemann, M., Johnston, M.G., Summers, W., et al. (2015a) Rice perception of symbiotic arbuscular mycorrhizal fungi requires the karrikin receptor complex. *Science* 350: 1521–1524.

Gutjahr, C., Radovanovic, D., Geoffroy, J., Zhang, Q., Siegler, H., Chiapello, M., et al. (2012) The half-size ABC transporters STR1 and STR2 are indispensable for mycorrhizal arbuscule formation in rice. *Plant J.* 69: 906–920.

Gutjahr, C., Sawers, R.J.H., Marti, G., Andrés-Hernández, L., Yang, S.Y., Casieri, L., et al. (2015b) Transcriptome diversity among rice root types during asymbiosis and interaction with arbuscular mycorrhizal fungi. *Proc. Natl. Acad. Sci. USA* 112: 6754–6759.

Handa, Y., Nishide, H., Takeda, N., Suzuki, Y., Kawaguchi, M. and Saito, K. (2015) RNA-Seq transcriptional profiling of an arbuscular mycorrhiza provides insights into regulated and coordinated gene expression in *Lotus japonicus* and *Rhizophagus irregularis*. *Plant Cell Physiol.* 56: 1490–1511.

Harrison, M.J. (2005) Signaling in the arbuscular mycorrhizal symbiosis. *Annu. Rev. Microbiol.* 59: 19–42.

Hogekamp, C., Arndt, D., Pereira, P.A., Becker, J.D., Hohnjec, N. and Küster, H. (2011) Laser microdissection unravels cell-type-specific transcription in arbuscular mycorrhizal roots, including CAAT-box transcription factor gene expression correlating with fungal contact and spread. *Plant Physiol.* 157: 2023–2043.

Hogekamp, C. and Küster, H. (2013) A roadmap of cell-type specific gene expression during sequential stages of the arbuscular mycorrhiza symbiosis. *BMC Genomics* 14: 306.

Hohnjec, N., Czaja-Hasse, L.F., Hogekamp, C. and Küster, H. (2015) Pre-announcement of symbiotic guests: transcriptional reprogramming by mycorrhizal lipochitooligosaccharides shows a strict co-dependency on the GRAS transcription factors NSP1 and RAM1. *BMC Genomics* 16: 994.

Hu, Z., Yan, H., Yang, J., Yamaguchi, S., Maekawa, M., Takamure, I., et al. (2010) Strigolactones negatively regulate mesocotyl elongation in rice during germination and growth in darkness. *Plant Cell Physiol.* 51: 1136–1142.

Jiang, L., Liu, X., Xiong, G., Liu, H., Chen, F., Wang, L., et al. (2013) DWARF 53 acts as a repressor of strigolactone signalling in rice. *Nature* 504: 401–405.

Kameoka, H. and Kyozuka, J. (2015) Downregulation of rice DWARF 14 LIKE suppress mesocotyl elongation via a strigolactone independent pathway in the dark. *J. Genet. Genomics* 42: 119–124.

Kawahara, Y., de la Bastide, M., Hamilton, J.P., Kanamori, H., McCombie, W.R., Ouyang, S., et al. (2013) Improvement of the *Oryza sativa* Nipponbare reference genome using next generation sequence and optical map data. *Rice* 6: 1–10.

Klingner, A., Bothe, H., Wray, V. and Marner, F.J. (1994) Identification of a yellow pigment formed in maize roots upon mycorrhizal colonization. *Phytochemistry* 38: 53–55.

Kobae, Y. and Fujiwara, T. (2014) Earliest colonization events of *Rhizophagus irregularis* in rice roots occur preferentially in previously uncolonized cells. *Plant Cell Physiol.* 255: 1497–1510.

Kobae, Y., Gutjahr, C., Paszkowski, U., Kojima, T., Fujiwara, T. and Hata, S. (2014) Lipid droplets of arbuscular mycorrhizal fungi emerge in concert with arbuscule collapse. *Plant Cell Physiol.* 55: 1945–1953.

Kobae, Y. and Hata, S. (2010) Dynamics of periarbuscular membranes visualized with a fluorescent phosphate transporter in arbuscular mycorrhizal roots of rice. *Plant Cell Physiol.* 51: 341–353.

Kobae, Y., Ohmori, Y., Saito, C., Yano, K., Ohtomo, R. and Fujiwara, T. (2016) Phosphate treatment strongly inhibits new arbuscule development but not the maintenance of arbuscule in mycorrhizal rice roots. *Plant Physiol.* 171: 566–579.

Kobae, Y. and Ohtomo, R. (2016) An improved method for bright-field imaging of arbuscular mycorrhizal fungi in plant roots. *Soil Sci. Plant Nutr.* 62: 27–30.

Koltai, H. (2014) Implications of non-specific strigolactone signaling in the rhizosphere. *Plant Sci.* 225: 9–14.

Koltai, H., LekKala, S.P., Bhattacharya, C., Mayzlish-Gati, E., Resnick, N., Wininger, S., et al. (2010) A tomato strigolactone-impaired mutant displays aberrant shoot morphology and plant interactions. *J. Exp. Bot.* 61: 1739–1749.

Kretzschmar, T., Kohlen, W., Sasse, J., Borghi, L., Schlegel, M., Bachelier, J.B., et al. (2012) A petunia ABC protein controls strigolactone-dependent symbiotic signalling and branching. *Nature* 483: 341–344.

Lin, H., Wang, R., Qian, Q., Yan, M., Meng, X., Fu, Z., et al. (2009) Dwarf27, an iron-containing protein required for the biosynthesis of strigolactones, regulates rice tiller bud outgrowth. *Plant Cell* 21: 1512–1525.

Liu, W., Kohlen, W., Lillo, A., Op den Camp, R., Ivanov, S., Hartog, M., et al. (2011) Strigolactone biosynthesis in *Medicago truncatula* and rice requires the symbiotic GRAS-type transcription factors NSP1 and NSP2. *Plant Cell* 23: 3853–3865.

López-Ráez, J.A., Charnikhova, T., Fernández, I., Bouwmeester, H. and Pozo, M.J. (2011) Arbuscular mycorrhizal symbiosis decreases strigolactone production in tomato. *J. Plant Physiol.* 168: 294–297.

López-Ráez, J.A., Fernández, I., García, J.M., Berrio, E., Bonfante, P., Walter, M.H., et al. (2015) Differential spatio-temporal expression of carotenoid cleavage dioxygenases regulates apocarotenoid fluxes during AM symbiosis. *Plant Sci.* 230: 59–69.

MacDonald, R.M. and Lewis, M. (1978) The occurrence of some acid phosphatases and dehydrogenases in the vesicular-arbuscular mycorrhizal fungus *Glomus mosseae*. *New Phytol.* 80: 135–141.

Maier, W., Peipp, H., Schmidt, J., Wray, V. and Strack, D. (1995) Levels of a terpenoid glycoside (blumenin) and cell wall-bound phenolics in some cereal mycorrhizas. *Plant Physiol.* 109: 465–470.

Marschner, H. (1995) Mineral Nutrition of Higher Plants, 2nd edn. Academic Press, London.

Minakuchi, K., Kameoka, H., Yasuno, N., Umehara, M., Luo, L., Kobayashi, K., et al. (2010) *FINE CULM1* (*FC1*) works downstream of strigolactones to inhibit the outgrowth of axillary buds in rice. *Plant Cell Physiol.* 51: 1127–1135.

Mosse, B. and Hepper, C. (1975) Vesicular arbuscular mycorrhizal infections in root organ cultures. *Physiol. Plant Pathol.* 5: 215–223.

Nadal, M. and Paszkowski, U. (2013) Polyphony in the rhizosphere: presymbiotic communication in arbuscular mycorrhizal symbiosis. *Curr. Opin. Plant Biol.* 16: 473–479.

Nadal, M., Sawers, R., Naseem, S., Bassin, B., Kulicke, C., Sharman, A., et al. (2017) An *N*-acetylglucosamine transporter required for arbuscular mycorrhizal symbioses in rice and maize. *Nat. Plant* 3: 17073.

Paszkowski, U., Kroken, S., Roux, C. and Briggs, S.P. (2002) Rice phosphate transporters include an evolutionarily divergent gene specifically activated in arbuscular mycorrhizal symbiosis. *Proc. Natl. Acad. Sci. USA* 99: 13324–13329.

Quinlan, A.R. and Hall, I.M. (2010) BEDTools: a flexible suite of utilities for comparing genomic features. *Bioinformatics* 26: 841–842.

Robinson, M.D., McCarthy, D.J. and Smyth, G.K. (2010) edgeR: a Bioconductor package for differential expression analysis of digital gene expression data. *Bioinformatics* 26: 139–140.

Salvioli, A., Ghignone, S., Novero, M., Navazio, L., Venice, F., Bagnaresi, P., et al. (2016) Symbiosis with an endobacterium increases the fitness of a mycorrhizal fungus, raising its bioenergetic potential. *ISME J.* 10: 130–144.

Sanders, F.E. and Sheikh, N.A. (1983) The development of vesicular-arbuscular mycorrhizal infection in plant root system. *Plant Soil* 71: 223–246.

Sasse, J., Simon, S., Gübeli, C., Liu, G.W., Cheng, X., Friml, J., et al. (2015) Asymmetric localizations of the ABC transporter PaPDR1 trace paths of directional strigolactone transport. *Curr. Biol.* 25: 647–655.

Schmitz, A.M. and Harrison, M.J. (2014) Signaling events during initiation of arbuscular mycorrhizal symbiosis. *J. Integr. Plant Biol.* 56: 250–261.

Seto, Y., Sado, A., Asami, K., Hanada, A., Umehara, M., Akiyama, K., et al. (2014) Carlactone is an endogenous biosynthetic precursor for strigolactones. *Proc. Natl. Acad. Sci. USA* 111: 1640–1645.

Smith, S.E. and Read, D.J. (2008) Mycorrhizal Symbiosis. Academic Press, Cambridge, UK.

Smith, S.E. and Smith, F.A. (2011) Roles of arbuscular mycorrhizas in plant nutrition and growth: new paradigms from cellular to ecosystems scales. *Annu. Rev. Plant Biol.* 63: 227–250.

Stirnberg, P., Furner, I.J. and Leyser, H.M.O. (2007) MAX2 participates in an SCF complex which acts locally at the node to suppress shoot branching. *Plant J.* 50: 80–94.

Sun, J., Nishiyama, T., Shimizu, K. and Kadota, K. (2013) TCC: an R package for comparing tag count data with robust normalization strategies. *BMC Bioinformatics* 14: 219.

Sun, J., Miller, J., Granqvist, E., Wiley-Kalil, A., Gobbato, E., Maillet, F., et al. (2015) Activation of symbiosis signaling by arbuscular mycorrhizal fungi in legumes and rice. *Plant Cell* 27: 823–838.

Sun, Z., Hans, J., Walter, M.H., Matusova, R., Beekwilder, J., Verstappen, F.W.A., et al. (2008) Cloning and characterisation of a maize carotenoid cleavage dioxygenase (*ZmCCD1*) and its involvement in the bio-synthesis of apocarotenoids with various roles in mutualistic and parasitic interactions. *Planta* 228: 789–801.

Takeda, N., Tsuzuki, S., Suzaki, T., Parniske, M. and Kawaguchi, M. (2013) CERBERUS and NSP1 of *Lotus japonicus* are common symbiosis genes that modulate arbuscular mycorrhiza development. *Plant Cell Physiol.* 54: 1711–1723.

Trapnell, C., Pachter, L. and Salzberg S.L. (2009) TopHat: discovering splice junctions with RNA-Seq. *Bioinformatics* 25: 1105–1111.

Umehara, M., Hanada, A., Magome, H., Takeda-Kamiya, N. and Yamaguchi, S. (2010) Contribution of strigolactones to the inhibition of tiller bud outgrowth under phosphate deficiency in rice. *Plant Cell Physiol.* 51: 1118–1126.

Umehara, M., Hanada, A., Yoshida, S., Akiyama, K., Arite, T., Takeda-Kamiya, N., et al. (2008) Inhibition of shoot branching by new terpenoid plant hormones. *Nature* 455: 195–200.

Vogel, J.T., Walter, M.H., Giavalisco, P., Lytovchenko, A., Kohlen, W., Charnikhova, T., et al. (2010) SlCCD7 controls strigolactone biosynthesis, shoot branching and mycorrhiza-induced apocarotenoid formation in tomato. *Plant J.* 61: 300–311.

Walker, N. and Smith, S.E. (1984) The quantitative study of mycorrhizal infection, II. The relation of rate of infection and speed of fungal growth to propagule density, the mean length of the infection unit and the limiting value of the fraction of the root infected. *New Phytol.* 96: 55–69.

Walter, M.H., Stauder, R. and Tissier, A. (2015) Evolution of root-specific carotenoid precursor pathways for apocarotenoid signal biogenesis. *Plant Sci.* 233: 1–10.

Waters, M.T., Gutjahr, C., Bennett, T. and Nelson, D.C. (2017) Strigolactone signaling and evolution. *Annu. Rev. Plant Biol.* 68: 8.1–8.31.

Xie, X., Yoneyama, K. and Yoneyama, K. (2010) The strigolactone story. *Annu. Rev. Phytopathol.* 48: 93–117.

Yao, R., Ming, Z., Yan, L., Li, S., Wang, F., Ma, S., et al. (2016) DWARF14 is a non-canonical hormone receptor for strigolactone. *Nature* 536: 469–473.

Yoshida, S., Kameoka, H., Tempo, M., Akiyama, K., Umehara, M., Yamaguchi, S., et al. (2012) The D3 F-box protein is a key component in host strigolactone responses essential for arbuscular mycorrhizal symbiosis. *New Phytol.* 196: 1208–1216.

Zhang, Y., van Dijk, A.D., Scaffidi, A., Flematti, G.R., Hofmann, M., Charnikhova, T., et al. (2014) Rice cytochrome P450 MAX1 homologs catalyze distinct steps in strigolactone biosynthesis. *Nat. Chem. Biol.* 10: 1028–1033.

Zhao, J., Wang, T., Wang, M., Liu, Y., Yuan, S., Gao, Y., et al. (2014) DWARF3 participates in an SCF complex and associates with DWARF14 to suppress rice shoot branching. *Plant Cell Physiol.* 55: 1096–1109.

Zhou, F., Lin, Q., Zhu, L., Ren, Y., Zhou, K., Shabek, N., et al. (2013) D14-SCF^{D3}-dependent degradation of D53 regulates strigolactone signalling. *Nature* 504: 406–410.